



Mechanistic deterioration by saponification of a 17th Century Oil Painting from the Museum of Modern Art in Cairo

Thanaa, A. Ali

Faculty of Archaeology, Aswan University,
Egypt

drthanaaabortaleb@arc.aswu.edu.eg

ABSTRACT

Metal soap plays a role in the deformation, fading, deterioration and cracking of oil paint layers as a result of the paintings being exposed to unsuitable environmental conditions. This leads to the interaction of metal ions with free fatty acids resulting from the hydrolysis of glycerides in the oil medium, or from protective varnish and forming metal soap, which catalyzes the hydrolysis of triglycerides in the oil medium and frees fatty acids. The decomposition of the medium then occurs and results in metal carboxylate, inside the coating film and precipitate on the surface of the painting, leading to damage. The mechanism of damage to oil paintings with lead-containing soap, characterized by long-chain elements of alkanes or chain soaps of lead (II), from octanoate to octadecenoate, has been analyzed using a 17th century oil painting from the Museum of Modern Art in Cairo. The analysis used a wide range of examination and analytical methods such as FTIR, Raman Spectroscopy, SEM-EDS, XRD, Gas chromatography (GC-MS), scanning electron microscopy, stereomicroscope, and examination with polarizing microscopy after making cross-sections. This is so that targeted strategies can be developed to slow deterioration at that particular stage and help determine the state of preservation of the artworks.

ARTICLE INFO

Article history

Received 15 January 2024

Received in revised form 04 April 2024

Accepted 17 April 2024

Available Online 17 April 2024

KEYWORDS

the saponification phenomenon;

Metal soap;

oil paintings;

Mechanistic deterioration.

INTRODUCTION:

Metal soap plays a role in the deformation, fading, deterioration, and cracks of the paint layers in oil paintings. The simultaneous presence of carboxylic acids in the oil medium and metal ions (lead, calcium, aluminum, or copper) in the paint results in the formation of long-chain metal carboxylate, known as metallic soap (Robinet 2003, 23.40). The identification of metal soaps has greatly increased in the past few years, along with the determination of their molecular and crystal structure, and their physical and chemical properties. (M. E. Cotte 2017, 2-23) (J. L. Hermans 2021, 22589-22600) (Helwig 2014, 87-167) (J. J. Hermans 2017, 9489-9496)

This phenomenon must be studied in order to formulate effective preservation methods to treat, stains and burrs that may cause coating layers to separate, especially for soap zinc (Sawicka 2014, 311-332) and, to a lesser extent, lead soap (M. C. Cotte 2007, 841-848). The presence of oxalates has been identified from the same minerals (N. S. Salvadó 2005, 3444-3451) (Sotiropoulou 2016, 559-567) in European collections of medieval woodcuts. Metal soap was discovered from lead and also from other minerals (for example, Zn, Cu (II), K, etc. in one of the paintings of the artist Rembrandt (Osmond 2012, 1136-1144) (J. J. Hermans 2019, 47-67). The lead soap forms bumps up to 200 microns in diameter, which may penetrate the surface of the lacquer, as in the case of the Madame X oil on canvas by J. S. Sargent (1884) where the varnish layers are translucent. Surface flakes form, and coating layers may become translucent and make support visible, as in Meindert Hobbema's Village among Trees (oil on a panel, 1670) (Lee 2018, 282-295).

Soap also leads to the formation of superficial crusts, as noted in the 17th century painting, a Portrait of a Woman by Jan van Ravestijn (M. C. Cotte 2007, 841-848). Studies since the 15th century have been carried out on hundreds of works of art affected by the phenomenon of soap resulting from inappropriate environmental factors such as exposure to light, changes in relative humidity, or high temperatures (Keune 2016, 448-457).

Metal soap on historical oil paintings as a result of the display in a changing climate and moisture leakage through the walls that migrate through the layers of the painting, starts with the linen fabric which absorbs moisture (Mayer 1999, 55-67) and leads to increased flexibility, and exposure to damage (Michalski 1991, 235-236). This effect is transmitted to the ground layer and leads to separation and fragmentation (Rachwał 2012, 474-481). The moisture is then transferred to the paint layer, especially the colors with heavy metals, with metallic soap appearing as a result of the interaction between the paint or drying agents (for example, white lead or litharge, cobalt, and copper) with the fatty acids when exposed to an alkaline environment and moisture (Chapman 1979, 77-79). The fatty acids result from decomposition of linseed oil (Britain 1988, 75-95) as well as the metal soap and is formed from interaction with beeswax or egg yolk (Liang 2014, 391-403) (N. B. Salvadó 2009, 419-428). The metal soap collects inside the paint layer (J. J. Hermans 2016, 10896-10905) to form aggregate blisters that grow and increase in size, which leads to cracking, and over time causes pressure on the painted layer turning them into pits (M. E. Cotte 2017, 2-23). Sometimes the metal soap migrates through the paint layers and gathers into blooms on the surface of the painting (Zucker 1999, 3-20), in addition to the "bump" phenomenon. It was found that metallic soap is associated with many other phenomena of deterioration. This is because the process is characterized by continuity and as a result of expansion and contraction, mechanical stresses occur that affect the mechanical properties of the colors. The result is that the hardness decreases and the blisters explode turning into pits, which causes the deterioration of the paint layer, increased fragility, loss of bonding strength, peeling and whitening (Ordonez 1997, 416-422). Blackness due to the increase in transparency is the precipitation of the color crust (Noble 2008, 68-78) (Boon 2008, 156-162) and the separation, cracks (Duffy 2014, 197-203). Some studies have indicated that the most common types of metallic soap found on oil paintings are, lead, zinc soaps. Copper soaps are rare and associated with green glazes and there are a few cases of potassium and calcium soaps.

Lead soap is the most common, due to the widespread use by artists of pigments containing white lead. $Pb(OH)_2$, $2PbCO_3$ $Pb(OH)_2$, lead tin lead type I, Pb_2SnO_4 lead soap, forms burrs of up to 200 microns in diameter that may penetrate the surface of the paint (Centeno 2009, 12-19). In the case of white lead, for example, it changes chemically, as it

turns into lead soap, and spreads through the paint layer, giving it a brown color (Centeno 2009, 12-19). The lead (II) soaps detected are mainly lead (II) hexadecanoate (palmitate), octadecanoate (stearate), or other unsaturated acids (oleate, linoleate, linolene). Lead and other metallic soaps (J. J. Hermans 2016, 10896-10905) in plaques are usually detected by infrared spectroscopy or diffraction (J. J. Hermans 2019, 10896-10905) (Centeno 2009, 12–19) (MacDonald 2016, 344-350). Using conventional techniques (P. Noble 2000, 126-129), metal carboxylate is difficult to detect in varnish layer cross-sections (Van der Weerd 2002, 275-283).

The main techniques used to determine paint components are Scanning Electron Microscopy (SEM) using Energy-Dispersive X-ray spectroscopy (EDX), and Gas Chromatography coupled with Mass Spectrometry (GC-MS). SEM-EDX gives access to the initial identification of pigments and inorganic additives, while GC-MS allows for the molecular identification of organic materials and varnishes. GC-MS in particular is a key tool for following chemical changes during oil drying (Mills 1966, 92-107). A wide variety of methods have been used to describe the degradation of soap in paintings and to study the reactions in typical paint samples such as spatially resolved techniques such as Raman spectroscopy and Fourier transform infrared (FTIR) spectroscopy (J. & Hermans 2020, 1505-1514).

1. Materials and Methods.

1.1 Materials

The study was carried out on an oil painting dated to the seventeenth century AD (artist unknown) from the holdings of the Museum of Modern Art in Cairo. The painting, which measures 80 cm in length and 50cm in width, is oil paint on a linen canvas, and is of a woman wearing a red, blue and white dress holding a glass bottle in her hand. The painting also has a 3D perspective drawn on a dark background. (Fig.1). The painting was stored in a dark and damp place in the museum and has various forms of damage, such as weakness and fragility of colors, cracks, peeling, and fading. Examination and analysis were carried out on two samples (one red and one blue) from the lady's colored dress that were falling from the painting (Fig.1).

1.2 Methods

Examination and Analysis

The study was carried out to analyze the materials used, and determine the structural composition of the painting.

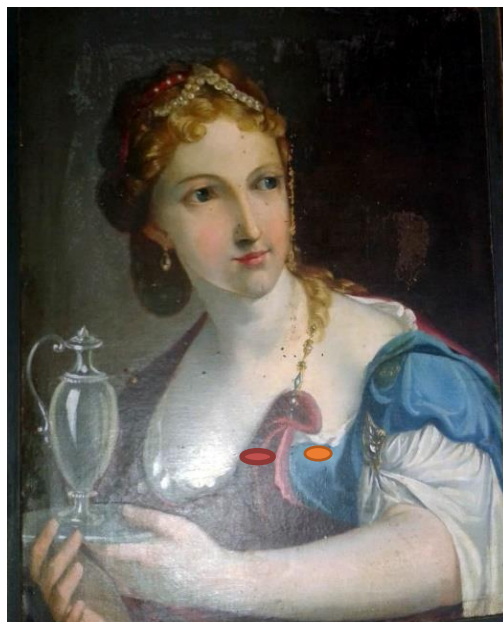


Fig.1 17th Century oil painting of a woman in a colored dress holding a glass bottle. The two sample locations are shown in red and orange. *Acknowledge where this photo comes from.*

1.2.1 Microscope and Visual Examination

Each sample was divided into two parts. One part for analysis and the other for examination as a cross section. The varnish layer was removed from the surface of the sample and the examination was done using a polarizing microscope Olympus BX50 Polarized Light Digital Microscope, and stereomicroscope (Olympus DP 731). Both microscopes were connected to a computer that had a camera magnification of 100x to identify the artist's technique, and surface damage.

1.2.2 Analysis by (SEM-EDX) and X-ray Diffraction Analysis XRD

The analysis by EDX aims to study the components of the paint and ground layer in the form of elements and the study of the surface appearance of the painting, and the nature of damage. The analysis was done at the Center for Metals and Mining in Helwan. The analysis by X-ray Diffraction (XRD) was done using a Philips X-Ray Diffraction machine, model type pw/1840 with Cu-k radiation and Ni-filter at 40 K V, 30 MA. Scanning speed 0.02/sec was used to find out the compounds that make up the paint and ground layer.

1.2.3 Fourier Transform Infra-Red Spectroscopy FTIR and Raman Spectroscopy

IR absorption spectroscopy is one of the basic methods used to identify the composition of molecules in their normal state. It can also be used to detect changes that occur to molecules as a result of damage and the formation of new molecules. The hard disk method was used, whereby the sample is blended into potassium bromide (KBr) and made into a hard disk. The weight of the sample in potassium bromide tablet (0.002g) is supplemented with a bromide disk up to (0.2g). Using a type device Agilent Technologies Cary 630 FTIR, analysis by Raman, is used to identify metal carboxylates which is a complementary technique for FTIR. Using Raman microscope type (SENTREEA π) and a 785 nm laser with a power of 10 microwatts for a period of 10 seconds.

1.2.4 Gas Chromatography Mass Spectrometry (GC-MS) analysis:

Checking the medium and carboxylate presence was analyzed by GC/MS, using a type Agilent Technologies 7890 A GC System, coupled with Agilent Technologies 5977 An MSD Mass Spectrometer. The GC-MS system was equipped with an HP-5ms GC/Agilent column (30 m × 0.32 mm i.e., 0.25 µm film thickness). Helium is used as a carrier gas at a flow rate of 1.0 mL/min and a split ratio of 1: 20 using the following temperature program: 80 C for 3 min; rising at 20 C/min to 180 C and held for 1 min, rising at 4 C/min to 220 C and rising at 20 C/min to 250 C and held for 5 min. 1µL of the mixtures were always injected. Mass spectra were obtained by electron ionization (EI) at 70 eV using spectral range of m/z 50-550. The identification of the chemical constituents of mixtures was de-convoluted using Agilent software and mass spectrum matching to the NIST library database.

2. Results and Discussion

2.1 The Microscope and Visual Examination

The results of the examination by a polarizing microscope of the light blue and red cross-section, showed that the layered structure of the painting comprised the linen canvas support, followed by one thin layer of ground, overlaid by two layers of paint. The paint was weak and suffered from stress and tension with blisters, bubbles, and cracks on the surface due to the appearance of metallic soap (Fig.2).

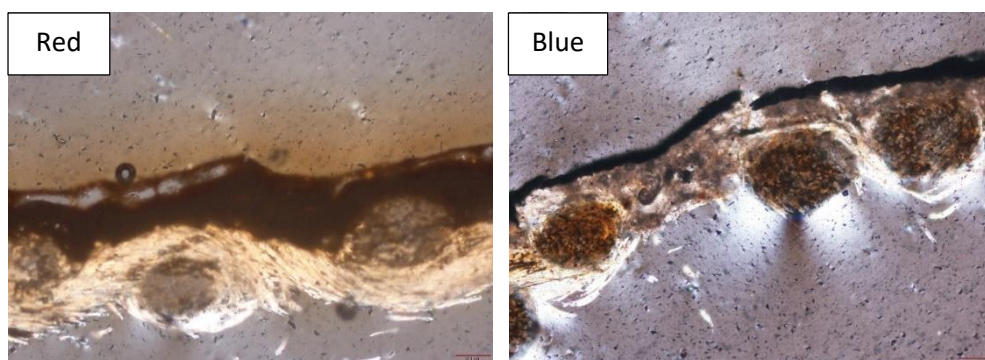


Fig.2 Examination by polarized light microscope (PLM) on the polished cross-sections of the red sample and blue sample showing the paint layer, which are very weak

The poor condition of the painting is the result of its interaction with moisture, which has caused swelling and shrinkage of the individual layers, and has led to internal stresses in the painting. These interactions led to a change in color and transparency, due to the chromatic change in humidity and results in efflorescence of salts on the surface of the paint and the formation of metallic soaps. The consequences are often disastrous for the integrity and appearance of the painting. Oblique light imaging showed cracks, protrusions, on the surface, and the color change as shown in figure 3A, with peeling, unevenness, and dirt on the surface, as shown in figure 3B.

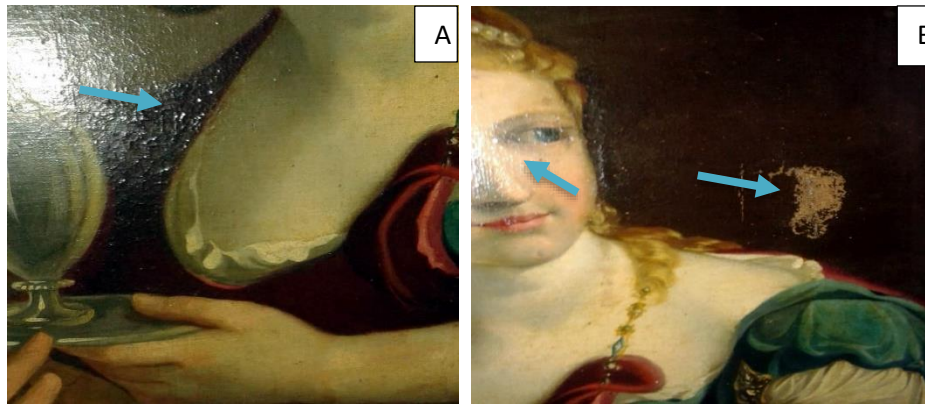


Fig.3 The Blisters on the surface, changing color, fig (A), The Peeling, Flaking, the uneven on the surface, fig (B)

The examination with a stereomicroscope showed the spread of blisters and cracks in the paint layer and a rough surface with bumps. These bumps grow below the paint layer and increase in size. This leads to the formation of prominent blocks that cover some parts of the painting and put pressure on the paint layer, leading to cracking or separation, or blisters explode and turn into pits. These effects cause deterioration and damage to the paint layer. The color of the surface changes, and there are gray and white area in the blue color (Fitzhugh 1997, 183-202) as shown in figure 4 and 5. The weakness of the red paint, separating, peeling off, and the appearance of cracks and holes leads to a rise between the layers, and the holes explode and form pits quickly, as shown in figure 6 and 7. The presence of white lumps differ in size and roughness on the surface.

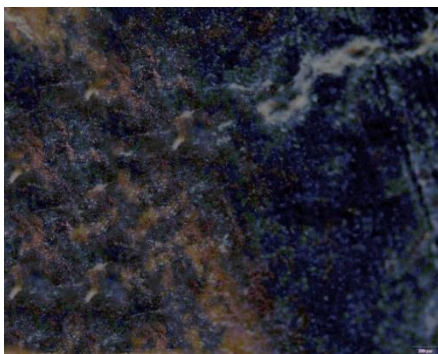


Fig.4 The decomposition paint, changing blue to gray and white

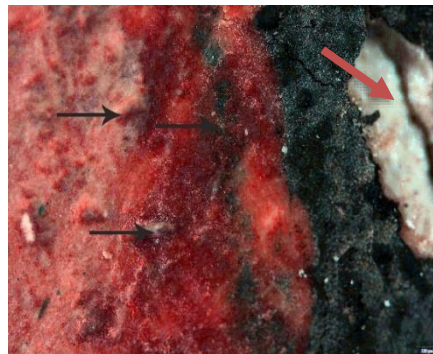


Fig.5 the Holes, blisters, metal soap, decomposition of binders

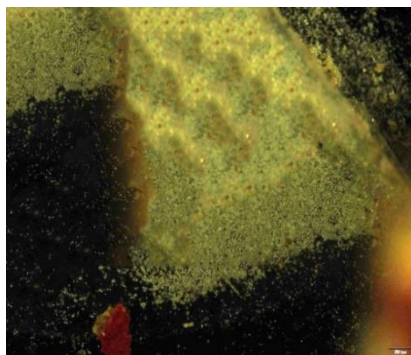


Fig.6 The dissolution of the paint layer and appeared a metal soap on surface



Fig.7 The protrusion and metallic soap appear on a blue paint layer

2.2 Analysis with (SEM-EDX) and XRD

Examination by SEM with a power of 2000x magnification showed that the paint layer suffers from severe weakness, corrosion and dirt, as shown in figure 8. With a magnification power of 4000x, the presence of white fragments and white lumps of different size that protrude on the surface and are completely distorted in the ground layers, as shown in figure 9.

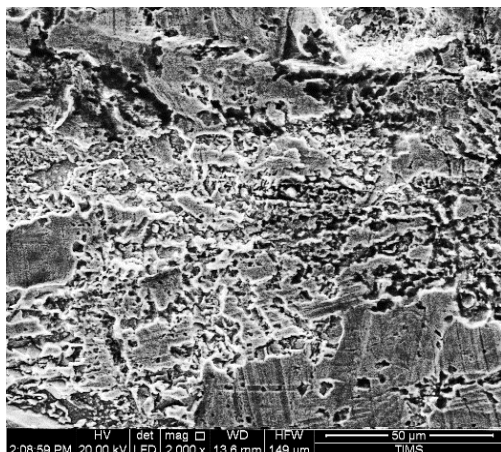


Fig.8 SEM at 2000X showing weakness, surface irregularities, dissolution of binders in blue sample

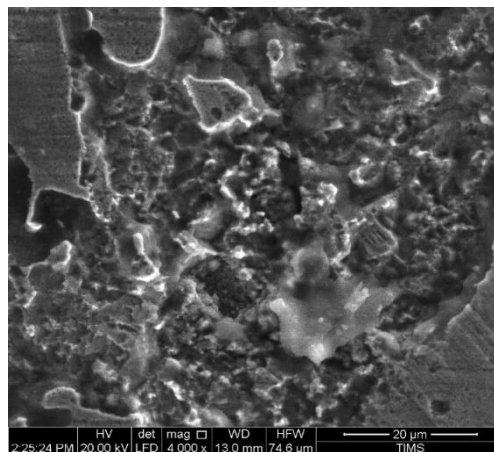


Fig.9 SEM at (4000X) showing weakness, dissolution, diffusion of metal atoms, in blue sample

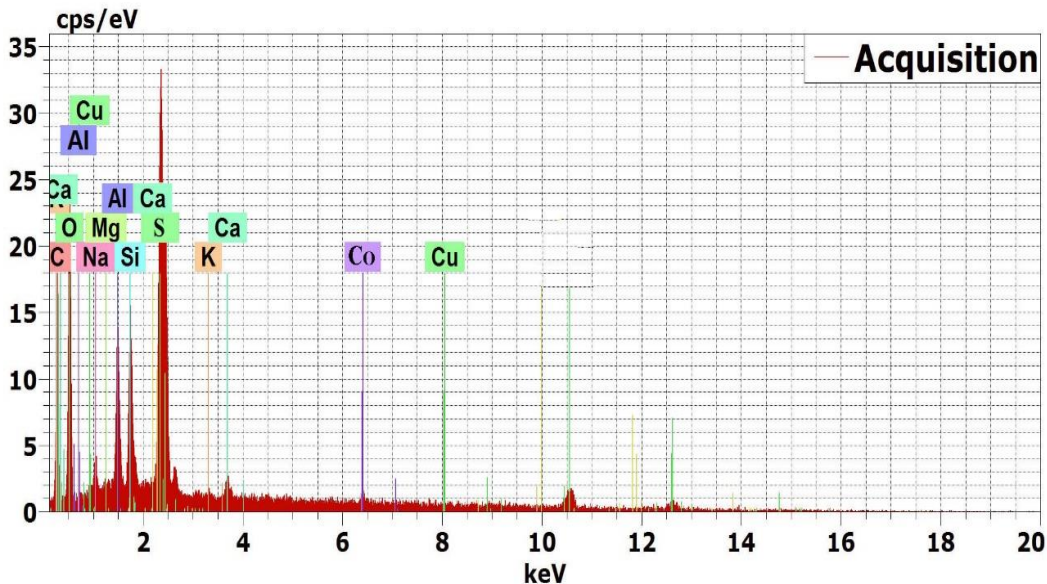


Fig.10 The EDX analysis of a blue paint sample

The analysis by EDX of the blue sample, as shown in figure 10, showed that the sample consisted of 7.85% copper, 3.53% silica, 3.57% sulfur, 4.06% aluminum, 4.61% calcium, 1.55% sodium, 0.07% potassium, 0.03% cobalt, and 0.23% magnesium. The color was confirmed as blue with XRD as azurite, which is composed of hydrated copper carbonates (Re 2011, 2373-2377). ($\text{Cu}_3(\text{CO}_3)_2(\text{OH})_2$ (Leyden 1991, 815-829), It is most probable that ultramarine blue was used as there was a presence of silica, aluminium, sulphur and potassium. This was mixed with the azurite blue to obtain shades of blue, and this was

confirmed by X-ray diffraction analysis, as shown in figure 11. This analysis also confirmed that the azurite blue constituted 16.6% of the color composition, ultramarine blue (sodalite) $[(Na,Ca)_8(Al,Si)_{12}O_{24}(S,SO_4)]$ at 18.6%, and hydrocite $C_2H_2O_8Pb_3$ at 0.9% , gypsum at 31.4%, calcite $CaCO_3$ at 27%, and spinel copper oxide at 5.4%. Examination of the red paint sample by SEM with a power of 4000-x magnification showed that the paint layer suffers from severe corrosion and decomposition, and the presence of white metallic soap lumps on the surface. These lumps differ in size, and are distorted as shown in figure 12 A and B. This analysis also showed blisters that had grown, which puts pressure on the paint layer, and leads to cracking and over time turning into pits. This causes deterioration of the paint layer, increased fragility, loss of bonding strength, peeling, and whiteness. The EDX analysis as shown in figure 13 confirmed that the red sample consists of 6.03% mercury, 5.61% calcium, 3.23% arsenic, 3.57% lead, 0.06% aluminum, 0.35% silica, 0.07% potassium, 0.37% iron, 0.03% copper, and 1.55% sodium. This shows that the red color is composed of a mixture of mercury

red with arsenic red and lead red, to obtain degrees of red color tone. The analysis was confirmed by X-ray diffraction as shown in figure 14 which showed the presence of vermilion at 1%, hematite at 3.5, Regular Red at 34.5%, lead red at 2.4%, galena (lead sulfide) at 0.6%, and calcite by 8.9%, and gypsum at 49.2%. Due to the presence of salts gypsum as a result of moisture on the ground layer, the colors that include lead compounds such as red lead oxide when exposed to air pollution such as sulfur oxide results in a black film of Lead dioxide and lead sulfide. The elemental map of the red sample by EDX, which shows the separation in the areas affected by soap in the paint layer is shown in figure 15.

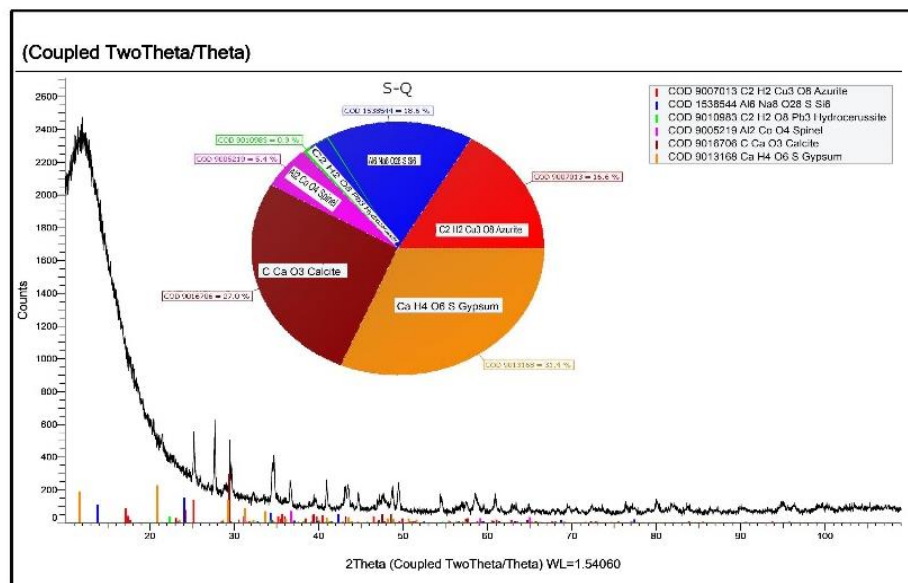


Fig.11 The X-ray diffraction analysis of a blue paint sample

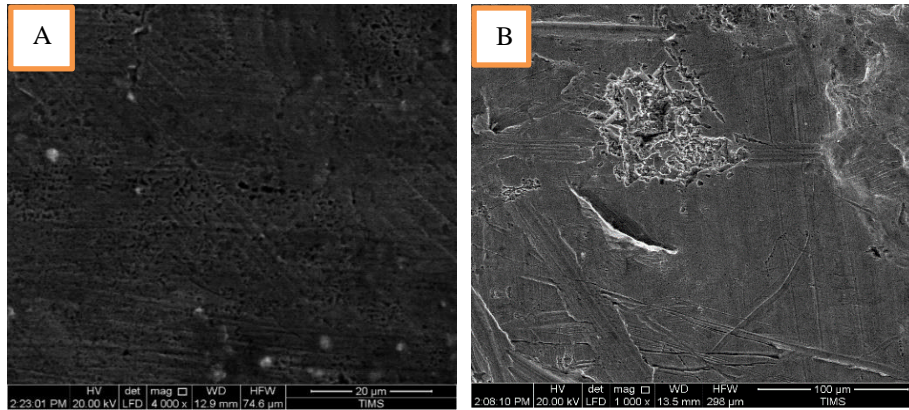


Fig.12 Examination by SEM in blue sample showing weakness, dissolution, diffusion of metal atoms, the appearance of metallic soap, magnification of 4000X (A), uneven surface, Holes, decomposition of paint, magnification of 2000X (B).

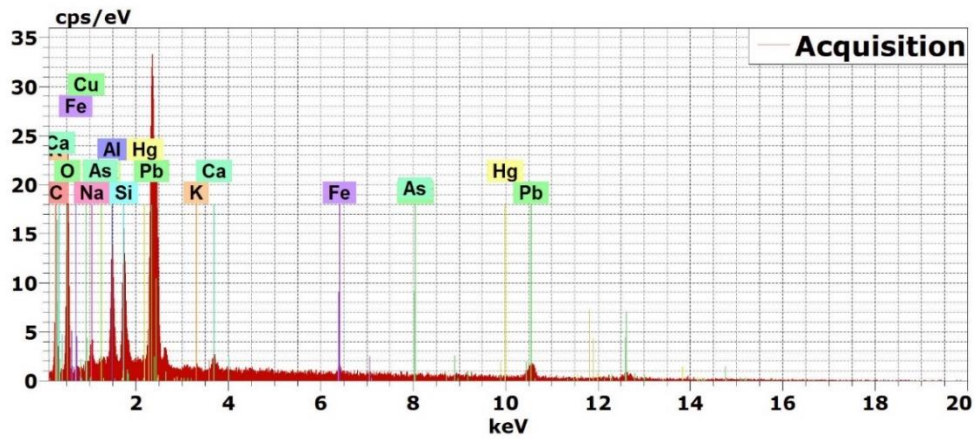


Fig.13 EDX analysis of the red paint sample

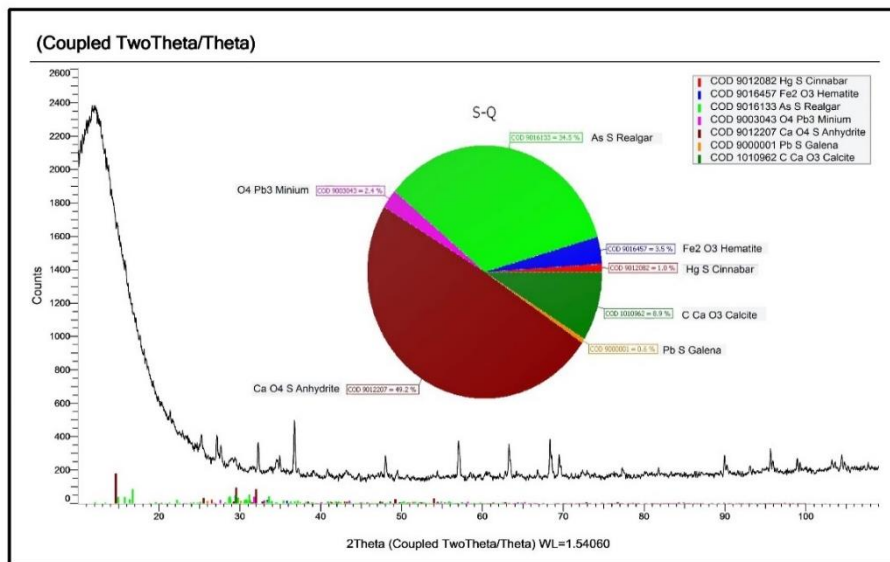


Fig.14 The analysis by X-ray diffraction for red paint sample

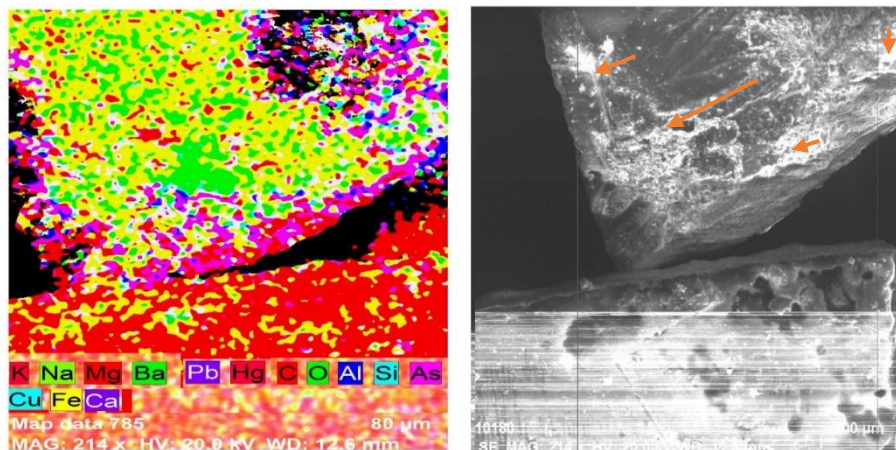


Fig.15 EDX element maps for the red paint sample

2.3 FTIR analysis and Raman spectroscopy

The FTIR analysis of the blue paint sample, which contained part of the ground layer, and the adhesive, is shown in figure 16. The presence of π -(CN stretching and NH bending) in the group at the wavenumber of 1585.13 cm^{-1} and the presence of a group (Amide I, C-O stretch), at a wavenumber of 1682.34 cm^{-1} , indicates that the adhesive is rabbit skin glue, and the appearance of spectra of glue mixed with calcium carbonate CaCO_3 at a wavenumber of 860.45 cm^{-1} for the carbonate (C-O) absorption group. The presence of the carbonate group at wavenumber of 1327.12 cm^{-1} , and 1458.79 cm^{-1} , suggests that the ground layer consists of calcium carbonate mixed with glue. The medium used in paint is linseed oil, due to the presence of a stretching band, O-H, at a wavenumber of 3364.12 cm^{-1} , C-H bending bands at a wavenumber of 2945.07 cm^{-1} , and a C=O (ester) stretching group at a wavenumber of 1735.12 cm^{-1} , and a wavenumber of 1421.65 cm^{-1} for the C-H bending bands, and the wavenumber at 1183.61 cm^{-1} and 1106.28 cm^{-1} for the C-O stretching bands. This suggests that the medium used was linseed oil (N. P.-S. Salvadó 2002, 215-222). The sodalite structure were found (Hoch 2005, 117-124) as there was a presence of absorption bands at a wavenumber in the range 1106.28 cm^{-1} and 924 cm^{-1} for the silica and aluminum silicate absorption group (Desnica 2004, 15-21), and the presence of absorption bands at a wavenumber in the range 1031.14 cm^{-1} · 906.74 cm^{-1} for the silicate group (Ramanaidou 2008, 129-156). The presence of absorption bands for the effective group of calcium oxalate salts (Van der Snickt 2011, 2216-2229) (Ca_2O_4) VS (CO) at the wavenumber of 1327.12 cm^{-1} and the presence of bands of absorption of metal soap and oxalate salts at the wavelength in the range of 1594.49 cm^{-1} . The analysis also indicated the presence of metal soap of the group (COO) at wavenumber of 1517.13 cm^{-1} , 1545.31 cm^{-1} , and 1585.13 (Silva 2006, 2183-2191) at wavenumber of 1458.79 cm^{-1} and 1421.65 cm^{-1} , the presence of aliphatic chains of fatty acids of the active group (CH_2) (De Laet 2013, 855-862) at wavenumber 2945.07 cm^{-1} . The analysis revealed the distinctive spectral features of azurite (Zaffino 2015, 1076-1085), $\text{Cu}_3(\text{CO}_3)_2(\text{OH})_2$, at wavenumbers of 3439.15 cm^{-1} , 1585.13 cm^{-1} , and 1458.79 cm^{-1} . and the presence of C-O group asymmetric stretches in the CO_3^{2-} at wavenumber of 1458.79 cm^{-1} and 1421.65 cm^{-1} and the presence of asymmetric stretching COO- group of a copper soap at wavenumbers of 1327.12 cm^{-1} and 860.45 cm^{-1} (N. B. Salvadó 2009, 419-428.) (N. B. Salvadó 2011, 3041-3052). The presence of copper carboxylate due to the presence of vas (CO) absorption group (Luxán 1999, 390-402) at the wavenumber of 1545.31 cm^{-1} and the presence of copper oxide, Cu-O skeleton stretching bands (Bruni 1999, 15-25), at the wavenumber of 860.45 cm^{-1} . The red sample analysis by FTIR showed the presence of an oil medium from linseeds due to the presence of the active group ($-\text{CH}$ stretch) at wavenumber 2925.98 and 2864.05 cm^{-1} and the active group ($-\text{C}=\text{O}$ stretch of

esterified and free fatty acids hydrolysed from the polymerized oil) at wavenumber 1735.12 and the presence of the active group (–C–O stretch) at wavenumbers of 1110.34 cm^{-1} and 1052.55 cm^{-1} as shown (Fig.17). The presence of the effective group of metal soap from lead carboxylate (N. B. Salvadó 2009, 419-428) (Mancilla 2009, 2050-2052) at wavenumbers 1640, 1544 resulting from hydrolyzed fatty acids and Pb^{2+} ions from lead red. These reactions occur where lead (II) ions in red lead interact with fatty acids in flax seed oil to form lead soap and metal soaps and existed at 1410. This usually occurs during the aging of oil paint, which contributes to the loss of chemical and physical properties. The presence of sulfate salts, SO_4^{2-} , was shown at a wavenumber of 659 cm^{-1} (Barman 2007, 5212-5217) revealed the presence of carboxylate as indicated by the COO– bands in the region of 1500-1600 cm^{-1} , as shown in figure 18.

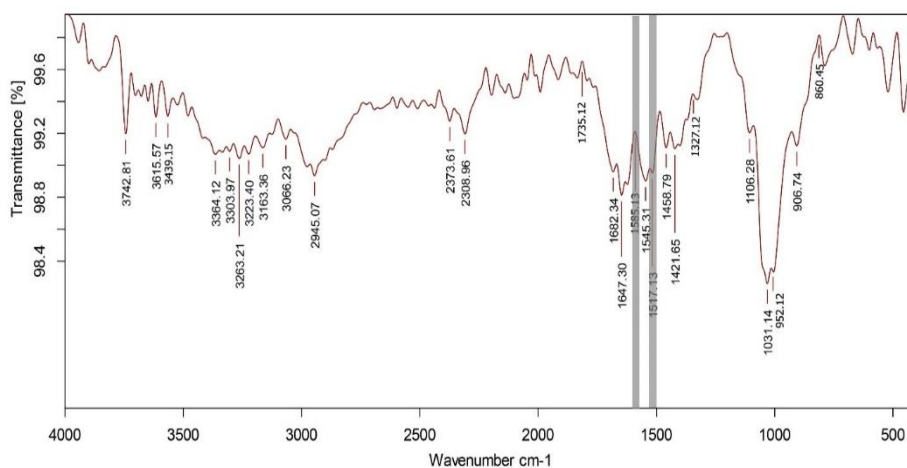


Fig.16 FTIR analysis of the blue paint sample

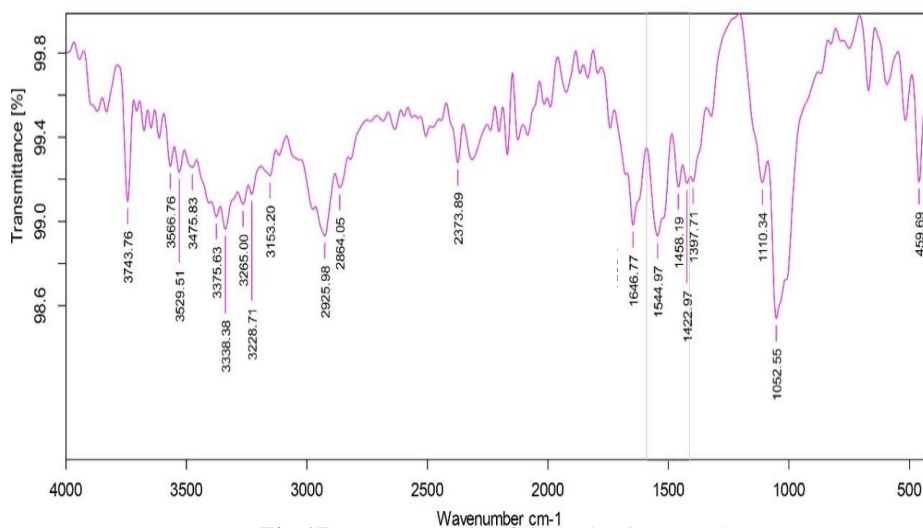


Fig.17 FTIR analysis of the red paint sample

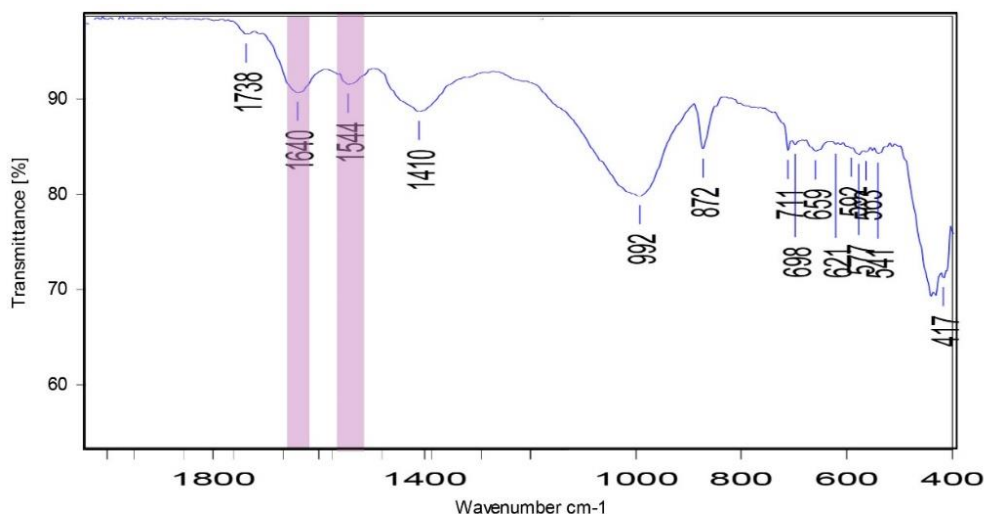


Fig.18 Carboxylate showed bands in the region of 1500-1600 cm^{-1} in FTIR.

Raman microscope analysis was done to confirm the infrared spectroscopy in the blue paint (Fig.19A and B) to characterize the metal carboxylates by detecting the carbon chains and cations that appeared in the Raman spectrum, in the range between 1210 - 862 cm^{-1} for mineral soaps and fatty acids respectively, The Raman spectra of metallic soap appeared in the region between 1706 and 231 cm^{-1} . In this range, the bands in the Raman spectrum of unsaturated fatty acids were identified at 1643 cm^{-1} -1677 cm^{-1} and the C-C stretching vibrations were determined, by distinguishing between the carbon chain lengths of both fatty acids and carboxylate-bound metals in the region between 1127 cm^{-1} and 1052 cm^{-1} . The bands in the Raman spectrum of palmitic acid and stearic acid were identified at 1086 cm^{-1} and 1113 cm^{-1} , respectively as shown in figure 19A, and Microscopy Raman spectroscopy with the magnification of lens 20x appear metallic soap is shown in figure 19B.

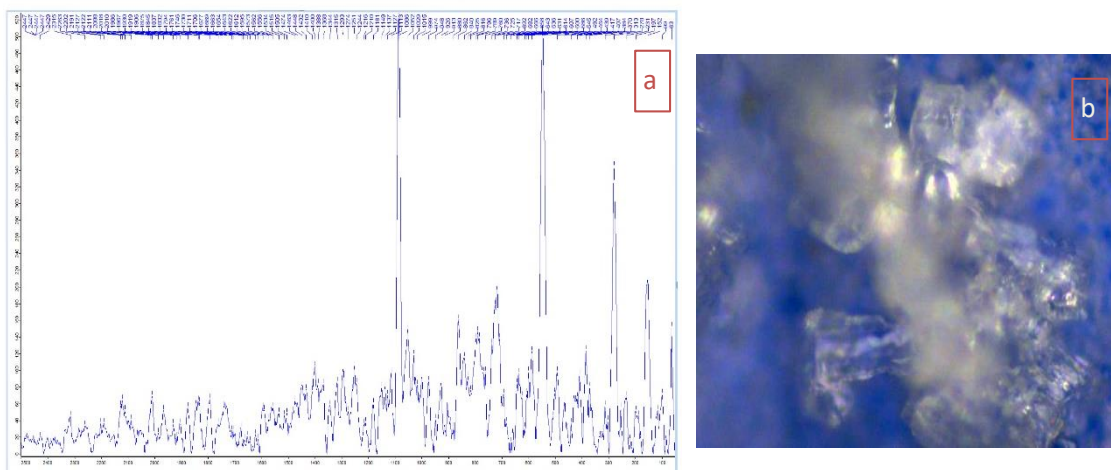


Fig. (19-a ,b) Raman spectra of blue paint (a), Microscopy Raman appear metal Soape (b)

2.4 GC-MS analysis

The GC/MS quantitative analysis showed the presence of carboxylic acids, which are the result of degradation, for example by lead soap, as shown in figure 20.

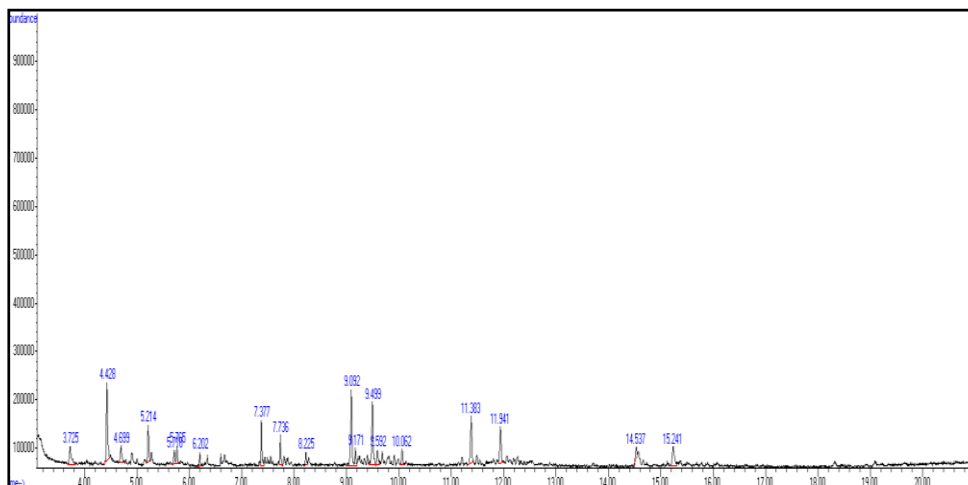


Fig.20 Carboxylate by GC-MS chromatograms analysis

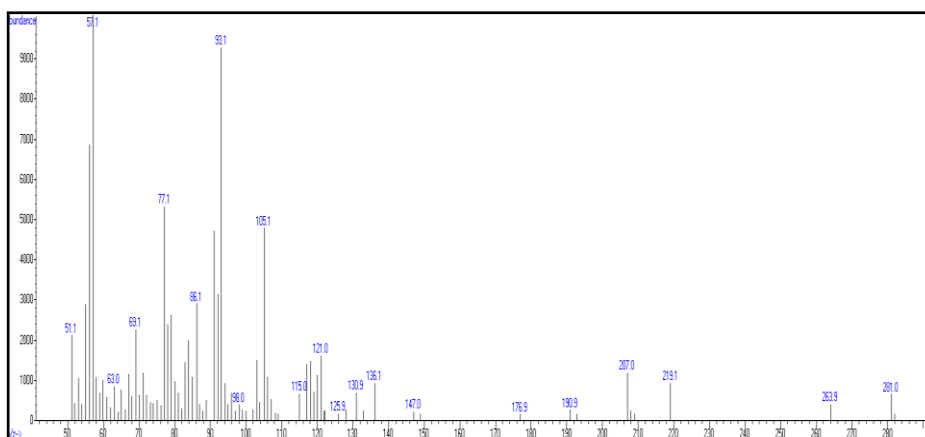


Fig.21 Medium by GC-MS chromatograms analysis

The medium for a sample, as shown in figure 21, showed a high levels of linolenic acid (C18:2) Content (51.21%) , linoleic (C18:3) Content (19.25%), and Oleic acid (C18:1) Content (18.51%), while the saturated acids were palmitic (C16:0) Content (6.58 %) and Stearic acid (C18:0) Content (4.43%), (Gruia 2012, 136-140) .

Polymerization by hydrolysis of the original parts of the triglycerides results in free fatty acids production (Mills 1966, 92-107, Bayrak 2010, 1836-1842). This process is stimulated by the presence of an acid or a strong base and moisture. Free fatty acids interact with colors that contain alkaline substances, including zinc, copper, and magnesium, tin, lead, and ferrous metals. Soluble alkaline substances from the colored materials are drawn on the surface and crystallize to form a precipitate.

Based on the results of the examinations and analysis carried out, the mechanism of damage can be explained as follows:

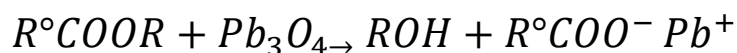
2.5 Saponification's Mechanism

Saponification's Mechanism of Action:

1- Entering an electron-hating (nucleophilic) group, which is the hydroxide group OH, to bind with the triglycerides.

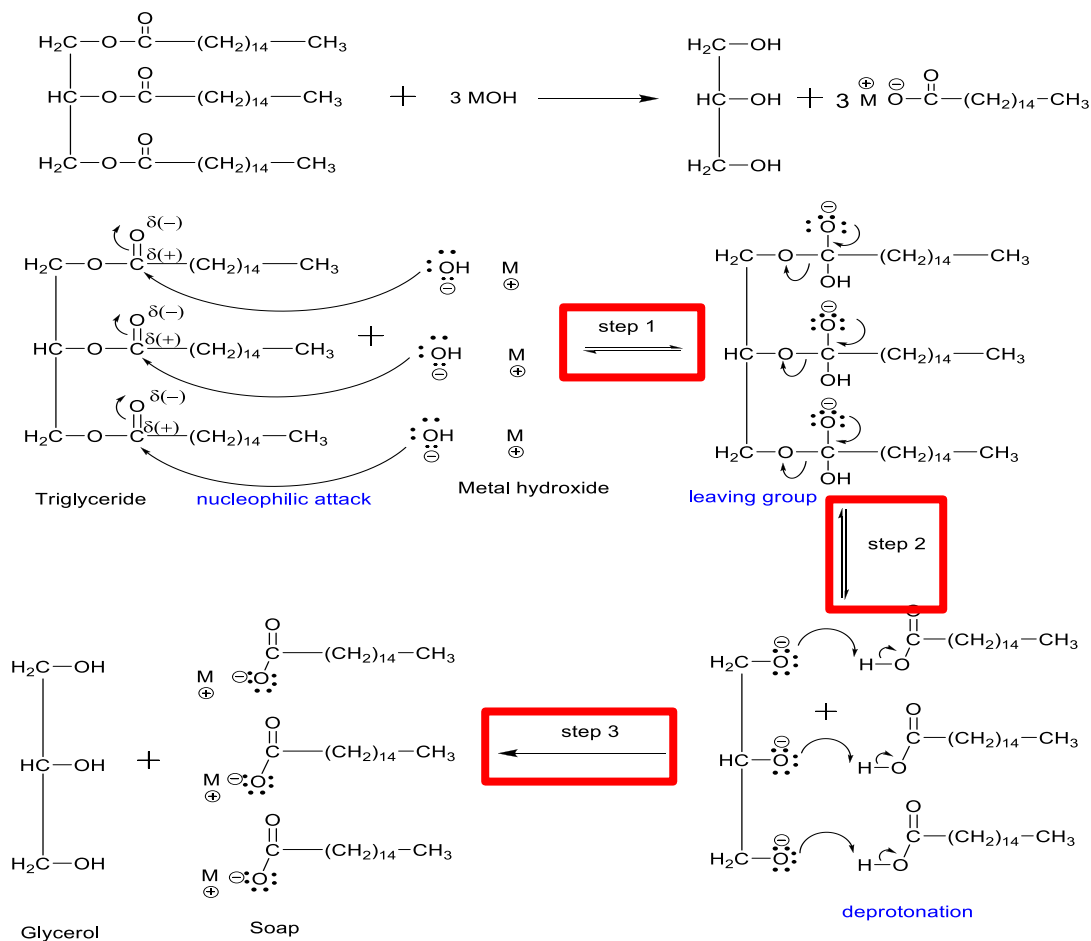
2 - The exit of the alkoxy group [which is an alkyl group (carbon and hydrogen chain) individually bonded to oxygen; Thus R–O [of a triglyceride compound.

3- Deprotonation of the hydroxide group attached to the triglycerides, so that this proton attaches to the free alkoxy group. At the end of this reaction, one molecule of glycerol and three molecules of the fatty acid salt (soap) will be produced, (scheme.1). (Fang 2018, 23-31)



Heavy metals used in pigments, such as those found in red lead, zinc white, lead white, and blue copper-containing pigment, react with the free fatty acids in the oil to produce glycerol and fatty acid salt (soap). Thus, μ SR-FTIR is particularly useful due to its micrometer-scale mapping ability. In order to distinguish the characteristic metallic soap bands, present between 1,200 and 1,800 cm^{-1} , ν (COO⁻), δ (CH₂), and ν (COO⁻), from other compounds present in paints, we need maximum discriminating power. Furthermore, the same minerals are also known to produce oxalates with strong absorption bands associated with the ν (C=O) carbonyl expansion in the same region. The main structures that were constructed, allowed for a higher level of confidence for the identification of copper palmitate and copper azelates for example in two Portuguese oil paintings from the 19th century (Otero 2014). These metal carboxylate surface interactions are expected to be a phenomenon also common to many pigments in polymerized linseed oil, as the coordination of metal ions on the surface of the pigment by carboxyl groups can help lower the interfacial energy between the pigment and the binding medium. Since metal ions are present in the polymeric binding medium, these same ions play a role in liberating fatty acids through hydrolysis, a proportion of which will be saturated.

Coatings with severe cracks show significant lead soap formation. If the coating is attacked by acids in its chemical environment, or anions, the relatively weak bond in the carboxylic acid can be broken. A carboxylic acid can lose its lattice connection and migrate, either separately or as a metal carboxylate. Thus, the transition through coating layers of fatty acids and metal carboxylates may occur.



Scheme.1 Mechanism of Saponification

Moreover, metal ions from the surface of selected paint or desiccants have been proposed to migrate through the polymer binding medium by hopping from one carboxylic acid to another. Migration of the mineral carboxylate causes a range of physical phenomena in the paintings, including bumps and inclusions that can be seen on the surface of paintings. It has also been observed that mineral carboxylate migrates without aggregation, moving toward the outer surface of the coating, where it reacts with atmospheric gases and remineralizers to form a crystalline shell (Van Loon 2011, 19-23).

Conclusions

Oil paintings are exposed to the metal soap phenomenon on the surface of the paint layer when exposed to an alkaline environment and high humidity. There are types metal soap found on paint layers, such as basic lead soap, and soap containing fatty acids and soap palmitates/esters. All different types have a color-destroying effect because they dissolve and react with paints that contain alkaline substances. The soluble alkaline substances are drawn from the paint substances to the surface, crystallize, and form a white, flaky precipitate, which leads to increased transparency, separation of the paint layers, especially in the white parts of paint materials that contain lead. Therefore, paintings must be preserved

by keeping them in appropriate environmental conditions, because mineral soap forms a layer that can significantly affect the appearance of the artwork.

Acknowledgment

I wish to thank Dr. Abu Al-Hamad, Head of the Chemistry Department, Aswan University Egypt for the opportunity to work with him.

Bibliography

- Barman, S., & Vasudevan, S. 2007. "Mixed saturated–unsaturated alkyl-chain assemblies: solid solutions of zinc stearate and zinc oleate." *The Journal of Physical Chemistry B* 19 (111): 5212-5217.
- Bayrak, A., Kiralan, M., Ipek, A., Arslan, N., Cosge, B., & Khawar, K. M. 2010. "Fatty acid compositions of linseed (*Linum usitatissimum* L.) genotypes of different origin cultivated in Turkey." *Biotechnology & Biotechnological Equipment*, 2 (24): 1836-1842.
- Boon, J. J., Van der Horst, J., Townsend, J., Doherty, T., & Heydenreich, G. 2008. "Preparation for Paintings." *The Artist's Choice and Its Consequences*. 156-162.
- Britain), National Gallery (Great. 1988. "(1988). National gallery technical bulletin." *Publications Department, National Gallery*. 12: 75-95.
- Bruni, S., Cariati, F., Casadio, F., & Toniolo, L. 1999. "Spectrochemical characterization by micro-FTIR spectroscopy of blue pigments in different polychrome works of art." *Vibrational Spectroscopy* 1 (20): 15-25.
- Centeno, S. A., & Mahon, D. 2009. "The chemistry of aging in oil paintings: metal soaps and visual changes." *The Metropolitan Museum of Art Bulletin* 1 (67): 12-19.
- Chapman, G. W. 1979. "Gas chromatographic determination of free fatty acids in vegetable oils by a modified esterification procedure." *Journal of the American Oil Chemists' Society*, 2 (56): 77-79.
- Cotte, M., Checroun, E., Susini, J., & Walter, P. 2007. "Micro-analytical study of interactions between oil and lead compounds in paintings." *Applied Physics* 1 (89): 841-848.
- Cotte, Marie, Elfi Checroun, Wilfried De Nolf, Yasuko Taniguchi, Léa De Viguierie, Michael Burghammer, et al. 2017. "Lead soaps in paintings: friends or foes?" *Studies in Conservation* 2-23.
- De Laet, N., Lycke, S., Van Pevenage, J., Moens, L., & Vandenberghe, P. 2013. "Investigation of pigment degradation due to acetic acid vapours: Raman spectroscopic analysis." *European Journal of Mineralogy*, 5 (25): 855-862.
- Desnica, V., Furić, K., & Schreiner, M. 2004. "Multianalytical characterisation of a variety of ultramarine pigments." *E-preservation science* 1: 15-21.
- Duffy, M., Martins, A., & Boon, J. J. 2014. "Metal soaps and visual changes in a painting by René Magritte—The Menaced Assassin." *Contemporary Oil Paint*, 197-203.
- Fang, Y. R., Yeh, Y., & Liu, H. S. 2018. "A novel strategy of biodiesel production from wet microalgae by direct saponification–esterification conversion (DSEC)." *Journal of the Taiwan Institute of Chemical Engineers* 23-31.
- Fitzhugh, E. W. 1997. "Artists' pigments: a handbook of their history and characteristics." *National Gallery of Art* 183-202.
- Gruia, A., Raba, D. N., Dumbrava, D., Moldovan, C., Bordean, D., & Mateescu, C. 2012. "Fatty acids composition and oil characteristics of linseed (*Linum Usitatissimum* L.) from Romania." *Journal of Agroalimentary Processes and Technologies* 2 (18): 136-140.
- Hearle, J. W., & Morton, W. E. 2008. "Physical properties of textile fibres." *Elsevier*.
- Helwig, Kate, Jennifer Poulin, Marie-Claude Corbeil, Elizabeth Moffatt, and Dominique Duguay. 2014. "Conservation Issues in Several Twentieth-Century Canadian Oil Paintings: The Role of Zinc Carboxylate Reaction Products." *Contemporary Oil Paint* (Springer International Publishing) 84-167.
- Hermans, J. J., Keune, K., van Loon, A., & Iedema, P. D. 2016. "The crystallization of metal soaps and fatty acids in oil paint model systems." *Physical Chemistry Chemical Physics* 16 (18): 10896-10905.
- Hermans, J. J., Keune, K., Van Loon, A., & Iedema, P. D. 2019. "Toward a Complete Molecular Model for the Formation of Metal Soaps in Oil Paints." *Metal Soaps in Art: Conservation and Research* 47-67.
- Hermans, J., & Helwig, K. 2020. "The identification of multiple crystalline zinc soap structures using infrared spectroscopy." *Applied Spectroscopy* 12 (74): 1505-1514.

- Hermans, Jan J. 2017. *Metal Soaps in Oil Paint: Structure, Mechanisms and Dynamics*. PhD thesis, Universiteit van Amsterdam.
- Hermans, Jan, Lieke Zuidgeest, Pieter Iedema, Sander Woutersen, and Koenraad Keune. 2021. "The Kinetics of Metal Soap Crystallization in Oil Polymers." *Physical Chemistry Chemical Physics* 23, (39): 22589-22600.
- Hobbema, M. 1985. *A View on a High Road*. National Gallery of Art.
- Hoch, M., & Bandara, A. 2005. "Determination of the adsorption process of tributyltin (TBT) and monobutyltin (MBT) onto kaolinite surface using Fourier transform infrared (FTIR) spectroscopy." *Colloids and Surfaces A: Physicochemical and Engineering Aspects* 1-3 (253): 117-124.
- Keune, K., Kramer, R. P., Huijbregts, Z., Schellen, H. L., Stappers, M. H., & van Eikema Hommes, M. H. 2016. "Pigment degradation in oil paint induced by indoor climate: comparison of visual and computational backscattered electron images." *Microscopy and Microanalysis*, 2 (22): 448-457.
- Lee, J., Bonaduce, I., Modugno, F., La Nasa, J., Ormsby, B., & van den Berg, K. J. 2018. "Scientific investigation into the water sensitivity of twentieth century oil paints." *Microchemical Journal* (138): 282-295.
- Leyden, D. E., & Atwater, J. B. 1991. "Hydrolysis and condensation of alkoxy silanes investigated by internal reflection FTIR spectroscopy." *Journal of adhesion science and technology* 5 (10): 815-829.
- Liang, J., & Scott, D. A. 2014. "Green-copper containing waxy paint on two Egyptian polychrome artifacts: a technical study." *Studies in Conservation* 6 (59): 391-403.
- Little, Carl, John Singer Sargent. 1998. "The Watercolors of John Singer Sargent." *Univ of California Press*.
- Luxán, M. P. D., & Dorrego, F. 1999. "Reactivity of earth and synthetic pigments with linseed oil." *Surface coatings international* 390-402.
- MacDonald, M. G., Palmer, M. R., Suchomel, M. R., & Berrie, B. H. 2016. "Reaction of Pb (II) and Zn (II) with ethyl linoleate to form structured hybrid inorganic-organic complexes." *a model for degradation in historic paint films. ACS omega* 1 (3): 344-350.
- Mancilla, N., D'Antonio, M. C., González-Baró, A. C., & Baran, E J. 2009. "Vibrational spectra of lead (II) oxalate. *Journal of Raman Spectroscopy: An International Journal for Original Work in all Aspects of Raman Spectroscopy. Including Higher Order Processes, and also Brillouin and Rayleigh Scattering* 12 (40): 2050-2052.
- Mayer, L., & Myers, G. 1999. "Bierstadt and other 19th-Century American painters in context." *Journal of the American Institute for Conservation* 1 (38): 55-67.
- Michalski, S. 1991. "Art in Transit: Studies in the Transport of Paintings, ch. Paintings—their response to temperature, relative humidity, shock, and vibration." *National Gallery of Art*.
- Mills, J. S. 1966. "The gas chromatographic examination of paint media. Part I. Fatty acid composition and identification of dried oil films." *Studies in Conservation* 2 (11): 92-107.
- Noble, P., Van Loon, A., Boon, J. J., Townsend, J., Doherty, T., & Heydenreich, G. 2008. "Preparation for Painting." *The Artist's Choice and its Consequences* 68-78.
- Ordóñez, E., & Twilley, J. 1997. "Peer reviewed: clarifying the haze." *efflorescence on works of art. Analytical chemistry* 13 (69): 416-422.
- Osmond, G., Boon, J. J., Puskar, L., & Drennan, J. 2012. "Metal stearate distributions in modern artists' oil paints: surface and cross-sectional investigation of reference paint films using conventional and synchrotron infrared microspectroscopy." *Applied Spectroscopy* 10 (66): 1136-1144.
- Otero, V., Sanches, D., Montagner, C., Vilarigues, M., Carlyle, L. Lopes, J. A., & Melo, M. J. 2014. "Characterisation of metal carboxylates by Raman and infrared spectroscopy in works of art." *Journal of Raman Spectroscopy* 11-12 (45): 1197-1206.
- P. Noble, J. Wadum, K. Groen, R. M. Heeren, K.-J. van den Berg. 2000. "in Proceedings of the International congress on contribution of chemistry to the works of art." *Art & Chimie, la couleur* 126-129.

- Rachwał, B., Bratasz, Ł., Krzemień, L., Łukomski, M., & Kozłowski, R. 2012. "Fatigue damage of the gesso layer in panel paintings subjected to changing climate conditions." *Strain* 6 (48): 474-481.
- Ramanaidou, B., Wells, M., Belton, D., & Ryan, C. 2008. "characterization of high-grade banded iron formation-derived iron ore." *REVIEWS IN ECONOMIC GEOLOGY* 129-156.
- Re, A., Giudice, A. L., Angelici, D., Calusi, S., Giuntini, L., Massi, M., & Pratesi, G. 2011. "Lapis lazuli provenance study by means of micro-PIXE. Nuclear Instruments and Methods in Physics Research Section B:." *Beam Interactions with Materials and Atom* 20 (269): 2373-2377.
- Robinet, Laurianne, and Marie-Claude Corbeil-a2. 2003. "Studies in conservation." 23-40.
- Salvadó, N., Butí, S., Labrador, A., Cinque, G., Emerich, H., & Pradell, T. 2011. "SR-XRD and SR-FTIR study of the alteration of silver foils in medieval paintings." *Analytical and bioanalytical chemistry* 3041-3052.
- Salvadó, N., Butí, S., Nicholson, J., Emerich, H., Labrador, A., & Pradell, T. 2009. "Identification of reaction compounds in micrometric layers from gothic paintings using combined SR-XRD and SR-FTIR." *Talanta* 2 (79): 419-428.
- Salvadó, N., Pradell, T., Pantos, E., Papiz, M. Z., Molera, J., Seco, M. E., & Vendrell-Saz, M. 2002. "Identification of copper-based green pigments in Jaume Huguet's Gothic altarpieces by Fourier transform infrared microspectroscopy and synchrotron radiation X-ray diffraction." *Journal of Synchrotron Radiation* 4 (9): 215-222.
- Salvadó, N., S. Butí, M. J. Tobin, E. Pantos, A. J. N. Prag, and T. Pradell. 2005. "Advantages of the Use of SR-FT-IR Microspectroscopy: Applications to Cultural Heritage." *Analytical Chemistry* 77 (11): 3444-3451.
- Sawicka, A., Burnstock, A., Izzo, F. C., Keune, K., Boon, J. J., Kirsch, K., and K. J. van den Berg. 2014. "An Investigation into the Viability of Removal of Lead Soap Efflorescence from Contemporary Oil Paintings." *Contemporary Oil Paint* 311-332.
- Silva, C. E., Silva, L. P., Edwards, H. G., & de Oliveira, L. F. C. 2006. "Diffuse reflection FTIR spectral database of dyes and pigments." *Analytical and bioanalytical chemistry* 2183-2191.
- Sotiropoulou, S., Z. E. Papliaka, and L. Vaccari. 2016. "Micro FTIR Imaging for the Investigation of Deteriorated Organic Binders in Wall Painting Stratigraphies of Different Techniques and Periods." *Microchemical Journal* 559-567.
- Van der Snickt, G., Miliani, C., Janssens, K., Brunetti, B. G., Romani, A., Rosi, F., ... & Wittermann, R. 2011. "Material analyses of 'Christ with singing and music-making Angels', a late 15th-C panel painting attributed to Hans Memling and assistants: Part I. non-invasive in situ investigations." *Journal of Analytical Atomic Spectrometry* 11 (26): 2216-2229.
- Van der Weerd, J., Brammer, H., Boon, J. J., & Heeren, R. M. 2002. "Fourier transform infrared microscopic imaging of an embedded paint cross-section." *Applied Spectroscopy* 3 (56): 275-283.
- Van Loon, A., Noble, P., & Boon, J. 2011. "White hazes and surface crusts in Rembrandt's Homer and related paintings." *In Preprints ICOM Committee for conservation 16th triennial meeting, Lisbon* 19-23.
- Zaffino, C., Guglielmi, V., Faraone, S., Vinaccia, A., & Bruni, S. 2015. "Exploiting external reflection FTIR spectroscopy for the in-situ identification of pigments and binders in illuminated manuscripts. Brochantite and posnjakite as a case study." *Spectrochimica Acta Part A: Molecular and Biomolecular Spectroscopy* 1076-1085.
- Zucker, J. 1999. "From the ground up: the ground in 19th-century American pictures." *Journal of the American Institute for Conservation* 3-20.

التدهور الميكانيكي عن طريق التصبين تطبيقاً للوحة زيتية من القرن السابع عشر من متحف الفن الحديث بالقاهرة

الملخص

يلعب الصابون المعدني دوراً في تشوه وبهتان وتدهور وتشقق الطبقة اللونية في اللوحات الزيتية نتيجة تعرض اللوحات لظروف بيئية غير مناسبة مما يؤدي إلى تفاعل أيونات المعادن مع الأحماض الدهنية الحرة الناتجة عن التحلل المائي من الجلسريدات بالوسيط الزيتي، أو من الورنيش الواقعي مما يؤدي إلى تشكيل الصابون المعدني ويحدث تحلل الوسيط الزيتي وتنتج منتجات التلف من الكربوكسيل المعدني، داخل طبقة الطلاء وتترسب على السطح وتؤدي إلى الضرر. سوف يتم وصف آلية تلف اللوحات الزيتية بالصابون المحتوي على الرصاص الذي يتميز بعناصر السلسلة الطويلة من الألكانات أو صابون الرصاص (II)، من الأوكتانوات إلى الأوكتاديكانات، باستخدام مجموعة واسعة من طرق التحليل مثل FTIR, Raman و SEM-EDS و XRD و كروماتوغرافيا الغاز (GC-MS) وطرق الفحص مثل الميكروسكوب الإلكتروني الماسح و الميكروسكوب الضوئي و الميكروسكوب المستقطب بعد عمل القطاعات العرضية وذلك حتى يمكن تطوير الاستراتيجيات المستهدفة لإبطاء التدهور للحفاظ على الأعمال الفنية.

ثناء علي علي

كلية الآثار،

جامعة أسوان

drthanaaobotaleb@arc.aswu.edu.eg

بيانات المقال

تاريخ المقال

تم الاستلام في

تم استلام النسخة المنقحة في

تم قبول البحث في

متاح على الإنترنت في

الكلمات الدالة

ظاهرة التصبين.

صابون معدني؛

لوحات زيتية؛

ميكانيكية التلف.